

Persistence and memory in patchwork dynamics for glassy models

Creighton K. Thomas,¹ Olivia L. White,² and A. Alan Middleton¹

¹*Department of Physics, Syracuse University, Syracuse, New York 13244, USA*

²*Department of Physics, Massachusetts Institute of Technology, Cambridge, Massachusetts 02139, USA*

(Received 31 January 2008; published 28 March 2008)

Slow dynamics in disordered materials prohibits direct simulation of their rich nonequilibrium behavior at large scales. “Patchwork dynamics” is introduced to mimic relaxation over a very broad range of time scales by directly equilibrating or optimizing on successive length scales. This dynamics is used to study coarsening and to replicate memory effects for spin glasses and random ferromagnets. It is also used to find, with high confidence, correct ground states in large toroidal samples.

DOI: [10.1103/PhysRevB.77.092415](https://doi.org/10.1103/PhysRevB.77.092415)

PACS number(s): 75.10.Nr, 05.10.-a, 75.50.Lk

The term “spin glass” refers to both experimental disordered magnetic systems and theoretical models with enough randomness and frustration in their interactions to preclude conventional magnetic order. The experimental systems exhibit a complex cluster of history-dependent nonequilibrium effects.^{1,2} For example, while a spin glass is “aged” at fixed temperature, its magnetic susceptibility slowly changes, even after it waits 20 orders of magnitude longer than the time for single spin reorientation. Upon further cooling, the material “rejuvenates:” its susceptibility reverts to what it would have been without the wait. Amazingly, the system does retain a “memory” of its history and, when temperature returns to that at which aging took place, susceptibility nears its aged value. In fact, waits at multiple temperatures can be stored and recovered.³ Similar effects are seen in a variety of experimental systems and multiple explanations have been proposed.^{2,4} Yet despite 30 years of study, the nature of spin-glass dynamics—and of aging and memory effects in other “glassy” materials—remains controversial and ill understood. In particular, how these effects are related to the temporal evolution of correlations is an open question.

In this Brief Report, we present “patchwork dynamics,” a numerical approach for studying the growth of correlations and nonequilibrium effects over a wide range of length and time scales in systems with quenched disorder. Patchwork dynamics proceeds by a succession of coarse-grained equilibrations—or optimizations at zero temperature—and provides a framework for investigating the relation between the evolution of microscopic correlations and the complex nonequilibrium effects observed in experimental spin glasses. This approach therefore replaces dependence on time by dependence on length scales. It can be used to study coarsening and the persistence of the initial state, to replicate memory and rejuvenation effects, to visualize how disordered systems store their history, and also as a ground state (GS) algorithm for systems that are otherwise difficult to optimize.

As an initial application, in this Brief Report, we investigate the two-dimensional (2D) Edwards–Anderson Ising spin-glass model (ISG) and the 2D random bond ferromagnet (RBFM), both at zero temperature. For both models, the Hamiltonian \mathcal{H} has the form $\mathcal{H} = -\sum_{\langle ij \rangle} J_{ij} s_i s_j$, where the Ising spin variables $s_i = \pm 1$ lie on a d -dimensional lattice and the J_{ij} are mean-zero Gaussian random variables for the ISG and are random, but positive, for the frustration-free RBFM

model. The nature of the low-temperature state in the ISG, including even the number of states, is still a subject of study^{5,6} and the response to perturbations, such as modifications of T , the J_{ij} , or boundary conditions (BCs), is complex and only partially understood. Note that the 2D ISG is glassy only as $T \rightarrow 0$, but we use it as a model for the low-temperature phase of glassy magnets where temperature is irrelevant. Patchwork dynamics is a general approach, with other immediate applications including⁷ nonequilibrium dynamics in three-dimensional (3D) spin glass models and 2D dimer models at finite temperature.

Dynamics in disordered materials is extremely slow since arbitrarily large groups of spins must rearrange to explore the low-free-energy phase space described by \mathcal{H} . A homogeneous ferromagnet (uniform positive J_{ij}) can move from any initial state to its ground state via energy lowering flips of small numbers of spins. By contrast, in a spin glass, arbitrarily large collective spin flips must occur.⁸ It has been argued that the case of the RBFM is similar: disorder pins domain walls, separating constant-spin domains on arbitrarily large scales.⁹ Furthermore, the time to flip a collection of spins grows quickly with the number of spins in the cluster. The associated time scale is $\sim \tau_0 e^{B/T}$, with τ_0 the microscopic time scale and B the energy barrier to the flip. For scale ℓ clusters, the typical barrier $B(\ell)$ will grow with the length scale, since more improbable events must simultaneously occur. The distribution of barriers will have a broad range of values and, thus, the distribution of flip times will be even more broadly distributed. Thus, a rough separation of time scales is expected for geometrically separated ℓ . In particular, this occurs for the simplest hypothesized scaling form $B \sim \ell^\psi$, with ψ a model-dependent scaling exponent and the width of the distribution of B given by its typical value. (Numerical evidence has sometimes suggested a power law growth,¹⁰ or logarithmic barriers, and the multiplicity of barriers also needs to be considered.) One numerical consequence is that the range of length scales that single-spin-flip Glauber dynamics can probe is severely limited by the quick growth of time scales with length, even though it can give some useful information about the evolution of correlations in spin glasses and other disordered systems.^{4,10,11}

The dependence of barriers on length scale motivates patchwork dynamics, which takes advantage of the separation of time scales to mimic the development of correlations. It operates over a succession of increasing spatial scales,

$\ell_m=1,2,\dots,2^m,\dots$, starting from an initial spin configuration on a given sample of fixed size L . For each m , we “equilibrate” the sample by optimizing (or equilibrating) randomly chosen subsystems—patches—of size ℓ_m , with fixed boundary conditions on a patch given by the surroundings. After applying sufficient patches at scale ℓ_m , the scale is increased to the next scale in the sequence, ℓ_{m+1} , and the procedure is repeated. (Results are similar for arithmetical sequences of ℓ_m .) We implement two versions of this dynamics. In the “complete” version, we repeat the optimization at each scale until no more improvements are possible. In the “mean coverage” approach, we apply $c(L/\ell_m)^d$ patches, where d is the physical dimension, covering the system c times at that scale. In both versions, patch placement is independent of the actual barriers, so the dynamics cannot replicate the fine-grained evolution of correlations. Refinements might include using a barrier-dependent success probability in placing patches or determining (nonsquare) patches that have the lowest estimated barrier.¹² Note that the general procedure is numerically tractable only when equilibration or optimization is fast enough at each length scale (for a review of methods, see, e.g., Ref. 13).

In spirit, patchwork dynamics resembles simulations used to study the mosaic picture of structural glass dynamics, where atoms are equilibrated inside a fixed shell, and analytic work on kinetically constrained models of glasses.¹⁴ Multiscale approaches have also been used to study spin glasses on hierarchical lattices¹⁵ as well as in optimization.¹⁶ However, here we focus primarily on using equilibrium or ground state solutions in the study of nonequilibrium dynamics.

We apply patchwork dynamics to study the equilibration of the 2D ISG Gaussian model and 2D RBFM model (with uniform distribution for $J_{ij} \in [0,1]$) on square lattices with toroidal BCs. We optimize each patch by using an exact ground state algorithm for fixed BCs.¹⁷ While we describe and carry out simulations for the case of optimization, equilibration on subsamples can replace ground states throughout. Calculations were carried out for systems up to size 256^2 , with patch sizes up to $\ell_m=128$, using on the order of 4×10^3 samples. The mean-coverage approach with $c=150$ is nearly indistinguishable from the complete approach and qualitative behaviors, including power law exponents for large ℓ_m , are independent of $c \geq 8$. Furthermore, the number of spins flipped at each scale approaches a c -independent limit, consistent with the assumption that changes over geometrically separated length scales occur on well-separated time scales.

To study the approach to the final state, at each scale ℓ_m we compare our solutions to the doubly degenerate optimal $T=0$ solution. For the RBFM, this configuration has uniform spin. For the ISG, we compare to the extended ground state¹⁷ the optimal combination of spin variables and choice of periodic or antiperiodic boundary conditions minimizing the Edwards-Anderson Hamiltonian, and we set boundary conditions accordingly. We estimate a coarsening length scale $b(\ell_m)$, as evident in Fig. 1, by the mean Manhattan distance from a randomly chosen point to a domain wall. We also compute the residual energy density $\delta e(\ell_m) = L^{-d}[E(\ell_m) - E_{GS}]$, where the overline indicates an average

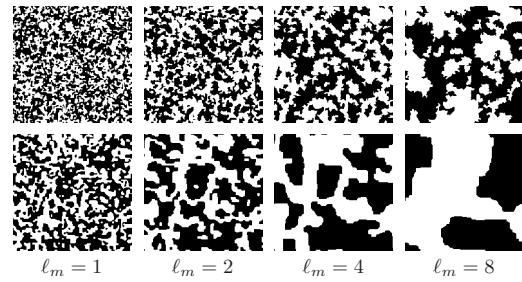


FIG. 1. Domain growth under patchwork dynamics for an $L^2 = 128^2$ sample. Light spins are aligned with one of the ground states, while dark spins are aligned with the other. The initial spins are random. At each scale ℓ_m , randomly selected patches of dimension $\ell_m \times \ell_m$ are optimized, with fixed spins exterior to the patch, until a stable configuration is reached. The upper row shows a history for the Ising spin glass, while the lower row is for the random bond ferromagnet, for which the typical domain size $b(\ell_m)$ grows faster than ℓ_m .

over disorder, $E(\ell_m)$ is the total Hamiltonian at the completion of the computations for stage m , and E_{GS} is the ground state energy for the sample. Figure 2 shows residual energy δe and domain size b as a function of patch scale ℓ_m . The spin-glass results are consistent with $\delta e \sim \ell_m^{\theta-2}$, with $\theta = -0.27$ (Ref. 18) and $b \sim \ell_m$. The results for the 2D RBFM are consistent with the expectation⁹ that $\delta e \sim \ell_m^{-4/3}$ and $b \sim \ell_m^{4/3}$. The accuracy of the slopes is about ± 0.1 in each case, with the expected power laws indicated by straight lines in Fig. 2.

In a spin glass, the decay of magnetization M from a fully magnetized initial condition is closely related to the persistence of a random initial spin configuration. Given a random initial condition, let $p(\ell_m)$ be the probability that a spin points in its $t=0$ direction. For a spin glass, the fully magnetized initial condition is random with respect to the bonds, so $M(\ell_m) = 2p(\ell_m) - 1$. Motivated by other known cases,¹⁹ Fisher and Huse⁵ conjectured that in the 3D EA model, $2p(\ell_m) - 1 \sim \ell_m^{-\lambda}$, where λ is an independent exponent describing the dynamics. A second exponent describing memory decay is the persistence exponent θ' ,^{19,20} where the probability that a spin has never flipped is conjectured to decay as $P(\ell_m) \sim \ell_m^{-\theta'}$.

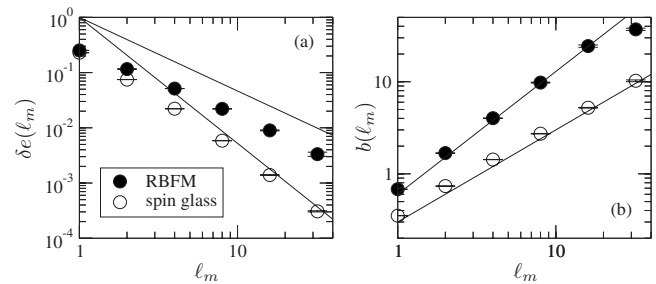


FIG. 2. Plots of (a) the residual energy density $\delta e(\ell_m)$ above the ground state energy density and (b) the domain scale $b(\ell_m)$, as a function of the patch size ℓ_m , for the 2D Ising spin glass and the random bond ferromagnet. Straight lines indicate power law behaviors described in the text.

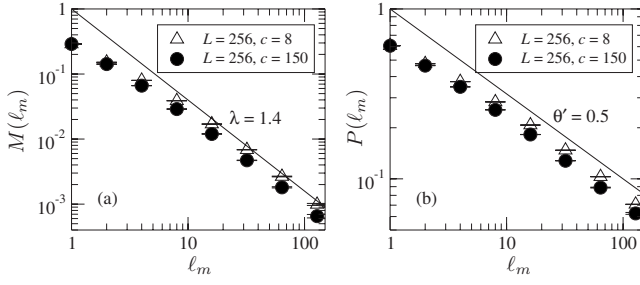


FIG. 3. Plot showing decay of the remanent magnetization and the persistence of the initial spin configuration in the Ising spin glass. The dependence of (a) magnetization $M(\ell_m)$ and (b) unflipped spins $P(\ell_m)$ are described by power laws with slopes of $-\lambda = -1.4 \pm 0.1$ and $-\theta' = -0.5 \pm 0.05$, respectively.

We use patchwork dynamics to investigate the values of λ and θ' in the ISG (Fig. 3). For $\ell_m > 16$, a power law decay describes the data well, with $\lambda_{SG} = 1.4 \pm 0.1$ and $\theta'_{SG} = 0.5 \pm 0.05$. Estimates of systematic rather than statistical error dominate total error. Details of the sequence of patch size do not affect our estimate of λ , as we have checked by applying patches at every scale, $\lambda = 1, 2, 3, \dots, L/2$. Furthermore, the effective exponents (slopes on log-log plots) are nearly independent of c for $L \geq 16$ and $8 < c < 150$. Similarly, for the RBFM, we find $\lambda_{RB} = 1.4 \pm 0.1$. Note that under patchwork dynamics, the boundaries of overlapping patches store memory since the dynamics optimizes (or equilibrates) all spins except those on the boundaries.

The dramatic rejuvenation and memory effects seen in temperature cycling experiments on spin glasses must arise from a special persistence.² The memory of magnetic susceptibility at a given temperature indicates that the pattern of magnetization must be encoded into the spin configuration and realized in physical space via domain growth at distinct temperatures. Similar memory effects are observed when the strength of exchange interactions are perturbed rather than the temperature.^{4,11,21} It is likely that this “disorder chaos” is related to “temperature chaos” and memory in experimental spin glasses. How disordered media such as spin glasses can retain spin information so effectively is a central issue in understanding their out of equilibrium behavior.

We use patchwork dynamics to investigate memory effects in the 2D ISG. Since there is no finite-temperature spin-glass phase, we perturb exchange interactions between “equilibrations.” We start with random initial conditions and couplings J_{ij} . First, we apply patches up to size $\ell_{\max}^{(1)}$. Second, we perturb bond strengths by an amount Δ , via $J_{ij} \rightarrow J'_{ij} = \frac{J_{ij} + \Delta K_{ij}}{\sqrt{1 + \Delta^2}}$, with K_{ij} -independent Gaussian random variables, and then we apply patches up to size $\ell_{\max}^{(2)}$. Finally, in the third stage, we revert to the J_{ij} and age using patches up to size $\ell_{\max}^{(3)}$. After steps $k=1, 2$, and 3 , the system configuration is denoted by $s_i(k)$. The two ground states with couplings J_{ij} and J'_{ij} are correlated on length scales smaller than the “chaos” length, $\xi \sim \Delta^{-1/\zeta}$, with $\zeta = d_s/2 - \theta \approx 0.91$.²² To quantify aging and memory effects, we use the sample-averaged spin overlap $q(k) = L^{-2} \sum_i s_i(1) s_i(k)$ for stages $k=2$ and 3 .

The full parameter space is four-dimensional, defined by

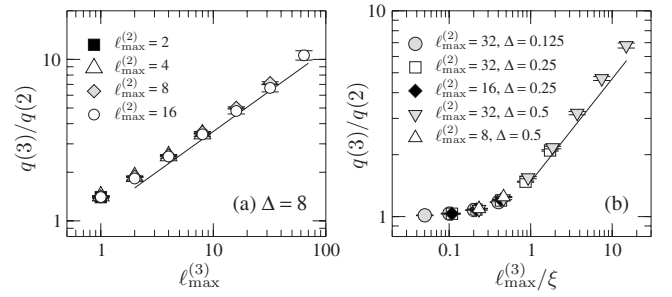


FIG. 4. Plots of the strength of memory in the 2D Ising spin glass at zero temperature, for strong and weak chaos. The first aging stage is long enough to reach the ground state for a given bond realization J_{ij} (with $L=128$). The system is coarsened under patchwork dynamics up to lengths $\ell_{\max}^{(2,3)}$ in stages 2 and 3, using bonds J'_{ij} and J_{ij} , respectively. (a) For large Δ , $\xi \approx 1.0$, and the final spin overlap $q(3)$ grows as $q(3)/q(2) \sim [\ell_{\max}^{(3)}]^\kappa$, with $\kappa = 0.5 \pm 0.05$, for $q(3)$ restricted to $q(3) < 0.5$. (b) For smaller Δ , using $\xi = 2.0(\Delta)^{-1/\zeta}$, and $\ell_{\max}^{(2)} > \xi$, $q(3)$ is constant until $\ell_{\max}^{(3)}$ exceeds ξ , and $q(3)/q(2)$ collapses to a single function of $\ell_{\max}^{(3)}/\xi$ [again, we restrict data to $q(3) < 0.5$]. Solid lines indicate $\kappa=0.5$.

$\ell_{\max}^{(1,2,3)}$ and Δ , so we focus on particular regions. We set $\ell_{\max}^{(1)} = \infty$, so that after the first stage, the system is in the ground state for the original couplings J_{ij} , giving $\ell_{\max}^{(1)} \gg \ell_{\max}^{(2,3)}$. We then investigate the two limits of large and small changes in exchange interactions, i.e., large and small Δ . For all memory simulations, we fix $c=50$.

When Δ is large, $\xi=1$ and the ground state for bonds J'_{ij} is nearly uncorrelated with that for bonds J_{ij} . Thus, the spin overlap after the second stage scales as $q(2) \sim [\ell_{\max}^{(2)}]^{-\lambda}$. During the third stage, we find that the overlap increases with increasing $\ell_{\max}^{(3)}$, as the ground state is recovered with the original J_{ij} . We find that $q(3)/q(2) \sim [\ell_{\max}^{(3)}]^\kappa$, with $\kappa = 0.5 \pm 0.05$, for $q(3) < 0.5$ and $8 \leq \ell_{\max}^{(3)} \leq 64$ [for $q(3) > 0.5$, the increase in $q(3)$ is independent of $q(2)$]. Figure 4(a) shows results for $\Delta=8$. In fact, there is no obvious difference in the behavior of $q(3)$ between the case where $\ell_{\max}^{(3)} < \ell_{\max}^{(2)}$ and the case where $\ell_{\max}^{(3)} > \ell_{\max}^{(2)}$.

We study the crossover from weak to strong chaos by using smaller values of Δ . The overlap length relating ground states for J_{ij} and J'_{ij} is $\xi \approx (2.00 \pm 0.15)\Delta^{1/\zeta}$. For $\ell_{\max}^{(2)} < \xi$, $q(2)$ is near unity. For $\ell_{\max}^{(2)} > \xi$, memory recovery in the third stage only occurs when $\ell_{\max}^{(3)} > \xi$. As shown in Fig. 4(b), the ratio $q(3)/q(2)$ plotted against $\ell_{\max}^{(3)}/\xi$ exhibits a convincing numerical collapse to a single function for $q(3) < 0.5$. The asymptotic memory growth is consistent with $q(3)/q(2) \sim [\ell_{\max}^{(3)}/\xi]^\kappa$.

Patchwork dynamics at $T=0$ also provides a simple and fast technique to quickly solve optimization problems¹⁶ in large systems or in systems on a toroidal lattice, which are, otherwise, difficult to study, especially for continuous disorder and arbitrary boundary conditions.^{10,17} Patchwork dynamics as a ground state heuristic can be seen as a variant of the variable neighborhood search method for optimal configurations.²³ Our particular method is very successful as it exploits the finite-dimensional structure of the spin-glass problem in physical space. For the 2D ISG on a toroidal lattice, by using fixed BC patches of size $L-1$ with coverage

$c=16$ and choosing the best evolved state from 20 random histories (a history is defined by an initial condition and patch placement sequence), we found the exact ground state in all of 10^3 samples of size $L=32$ and $L=64$. For larger systems, we do not have access to an exact solution to test the heuristic except in the case where the ground state is equal to the extended ground state.¹⁷ In such cases, we find the exact ground state in all of 10^4 samples of size $L=256$. The mean time to find the ground state is approximately 1.5 histories. Even by using smaller patches of size $L/2$ and $c=50$ in systems of size $L=128$, we found the exact extended ground state on a torus using 120 histories with no failures in all of the 10^4 samples; therefore, half-size patches can be used to find the ground state. Such techniques are currently being studied to compute precise exponent values for the 2D ISG and to increase the size of 3D systems that can be studied with high confidence.⁷

In conclusion, a coarse-grained evolution on a sequence

of length scales mimics the long time scales associated with nonequilibrium evolution in disordered systems, greatly reducing computational time and also providing a theoretical framework for studying nonequilibrium effects in such systems. We demonstrate the use of this approach in determining coarsening and persistence exponents, finding exact ground states in practice, and replicating aging and memory effects. One important further application is to extend these investigations to 3D Ising spin glasses.⁷ Additionally, the use of this dynamics could be coupled with hierarchical approaches for estimating barriers in glassy models.¹²

This work was supported in part by NSF Grant No. DMR 0606424. We thank Daniel Fisher for stimulating discussions, Frauke Liers for confirming our results on exact ground states on toroidal systems, and the Aspen Center for Physics for its hospitality.

-
- ¹ *Spin Glasses and Random Fields*, edited by A. P. Young (World Scientific, Singapore, 1998); K. Binder and A. P. Young, *Rev. Mod. Phys.* **58**, 801 (1986); S. F. Edwards and P. W. Anderson, *J. Phys. F: Met. Phys.* **5**, 965 (1975).
- ² E. Vincent, *Ageing and the Glass Transition*, edited by M. Henkel, M. Pleimling, and R. Sanctuary (Springer, Berlin, 2007).
- ³ S. Miyashita and E. Vincent, *Eur. Phys. J. B* **22**, 203 (2001).
- ⁴ P. E. Jönsson, R. Mathieu, P. Nordblad, H. Yoshino, H. A. Katori, and A. Ito, *Phys. Rev. B* **70**, 174402 (2004).
- ⁵ D. S. Fisher and D. A. Huse, *Phys. Rev. B* **38**, 373 (1988).
- ⁶ M. Mezard, G. Parisi, and M. Virasoro, *Spin Glass Theory and Beyond* (World Scientific, Singapore, 1987); M. Palassini and A. P. Young, *Phys. Rev. Lett.* **85**, 3017 (2000); F. Krzakala and O. C. Martin, *ibid.* **85**, 3013 (2000).
- ⁷ C. K. Thomas, O. L. White, and A. A. Middleton (unpublished).
- ⁸ C. M. Newman and D. L. Stein, *Phys. Rev. E* **60**, 5244 (1999); C. M. Newman and D. L. Stein, *Phys. Rev. Lett.* **82**, 3944 (1999).
- ⁹ D. A. Huse and D. S. Fisher, *Phys. Rev. Lett.* **57**, 2203 (1986).
- ¹⁰ R. Paul, G. Schehr, and H. Rieger, *Phys. Rev. E* **75**, 030104(R) (2007); J. Kisker, L. Santen, M. Schreckenberg, and H. Rieger, *Phys. Rev. B* **53**, 6418 (1996).
- ¹¹ H. Yoshino, A. Lemaitre, and J.-P. Bouchaud, *Eur. Phys. J. B* **20**, 367 (2001); H. Yoshino, *J. Phys. A* **36**, 10819 (2003).
- ¹² C. Amoruso, A. K. Hartmann, and M. A. Moore, *Phys. Rev. B* **73**, 184405 (2006).
- ¹³ A. Hartmann and H. Rieger, *Optimization Algorithms in Physics* (Wiley-VCH, Berlin, 2001).
- ¹⁴ A. Cavagna, T. S. Grigera, and P. Verrocchio, *Phys. Rev. Lett.* **98**, 187801 (2007); R. L. Jack and J. P. Garrahan, *J. Chem. Phys.* **123**, 164508 (2005).
- ¹⁵ M. Sasaki and O. C. Martin, *Phys. Rev. Lett.* **91**, 097201 (2003); F. Scheffler, H. Yoshino, and P. Maass, *Phys. Rev. B* **68**, 060404(R) (2003).
- ¹⁶ J. Houdayer and O. C. Martin, *Phys. Rev. Lett.* **83**, 1030 (1999).
- ¹⁷ C. K. Thomas and A. A. Middleton, *Phys. Rev. B* **76**, 220406(R) (2007).
- ¹⁸ I. A. Campbell, A. K. Hartmann, and H. G. Katzgraber, *Phys. Rev. B* **70**, 054429 (2004).
- ¹⁹ A. J. Bray, *Adv. Phys.* **43**, 357 (1994).
- ²⁰ B. Derrida, A. J. Bray, and C. Godreche, *J. Phys. A* **27**, L357 (1994).
- ²¹ H. G. Katzgraber and F. Krzakala, *Phys. Rev. Lett.* **98**, 017201 (2007); L. Berthier and A. P. Young, *Phys. Rev. B* **71**, 214429 (2005).
- ²² A. J. Bray and M. A. Moore, *Phys. Rev. Lett.* **58**, 57 (1987); F. Krzakala and J.-P. Bouchaud, *Europhys. Lett.* **72**, 472 (2005); H. Rieger, L. Santen, U. Blasum, M. Diehl, M. Jünger, and G. Rinaldi, *J. Phys. A* **29**, 3939 (1996).
- ²³ P. Festa, P. M. Pardalos, M. G. C. Resende, and C. C. Ribeiro, *Optim. Methods Software* **17**, 1033 (2002).